ChemComm
FEATURE ARTICLE

Understanding structure and reactivity of new fundamental inorganic molecules: metal sulfides, metallocarbohedrenes, and nitrogenase

Ian Dance

School of Chemistry, University of New South Wales, Sydney 2052, Australia

A large number of new and unexpected molecules, fundamentally inorganic and containing just metal and sulfur, or metal and carbon, can be synthesised in the gas phase, and their reactivities investigated. In the absence of bulk samples and definitive characterisation data they can be very profitably investigated using density functional calculations. A valuable perspective places these new and unprotected molecules in the context of related non-molecular solids, and terminally ligated molecules. The Fe_7MoS_9 cluster which effects the mild reduction of N_2 at the active site of nitrogenase is similarly undercoordinated, floppy, and reactive. Density functional calculations reveal the characteristics of the Fe_7MoS_9 site and elucidate postulated mechanisms for the reduction.

Introduction

Consider this experiment: cobalt sulfide, as the familiar black insoluble solid, is energised with a high power pulse of a 1064 nm laser, in a high vacuum chamber. A plasma occurs at the surface, and after collisional cooling the products formed are trapped as negative ions, and assayed mass spectrometrically. The resulting mass spectrum reveals 83 binary species $[Co_xS_y]^-$, ranging in size up to $[Co_{38}S_{24}]^-$.[1]

What have we done? We have prepared 83 structurally-molecular forms of a fundamental inorganic binary compound, cobalt sulfide, which previously had been known only with non-molecular structure. This experiment is the metal sulfide analogue of the better known laser ablation of a non-molecular allotrope of carbon (graphite) to generate the family of fullerenes, which are elemental carbon in molecular form.

This feature article is about newly discovered inorganic molecules which are comprised of just two (or at most a few) elements, and yet which are unprecedented in composition and structure and reactivity. These molecules are at the core of inorganic chemistry, but they do not adhere to the traditional notions of composition or oxidation state or valence, and they require new concepts of structure and bonding. Very often these new molecules have their genesis in the gas phase (like the fullerenes). However, as described below, metal sulfide cores are also deployed by evolved biological chemistry to effect significant reactivity which is beyond current human capability in the laboratory.

Molecular binary metal chalcogenides

By gas phase experiments like that already outlined, the generation of metal sulfide (and selenide and telluride) molecular clusters $[M_xE_y]^-$ has been achieved for all of the first row transition metals, and others.[2–4] We know that these new molecules are formed in the gas phase by associative processes involving atoms, ions and/or electrons generated in a high energy plasma, and that our experiment does not merely excise various fragments from the solid metal sulfide. This conclusion derives from the result that the distributions of product ions are largely independent of the properties of the solid precursor, and the fact that laser ablation of a mixture of elemental copper and selenium gives the same distribution as copper selenide precursors.[5,6] Through this experimental program we now know of the existence of many hundreds of unprecedented molecular metal sulfides $[M_xS_y]^-$, and have information about their relative abundances, stabilities, and reactivities.[1,2,4,6–13]

Before considering the position of these metal sulfide molecules in the menagerie of chemistry, it is worth mentioning a related inorganic experiment also performed in the cell of the Fourier transform ion cyclotron resonance (FTICR) mass spectrometer: this cell can be regarded as a gas-phase 'beaker', in which we can undertake controlled synthesis and purification of new species, and investigate their reactivities, reactions, and dissociations.[13,14] All of the metals (except Tc) can be isolated as M^+ in this cell, and reacted with the elemental reagent $S_{8\,(g)}$, forming numerous cations $[MS_n]^+$. This is comparative inorganic chemistry *par excellence*: it compares all metals, in the same oxidation state, reacting with the same reagent under the same conditions.[14,15]

Inorganic perspectives: non-molecules, exposed molecules, and protected molecules

What structural perspective best serves the numerous questions which arise for these and related newly discovered molecules? A threefold overall classification is valuable. At one extreme are binary and ternary compounds which are structurally non-molecular (in one, two or three dimensions) and which therefore occur only in the solid state, and for which detailed structural data are available crystallographically. At the other extreme are conventional molecular compounds in which a metal cluster core is terminally ligated by ligands: this is the class of 'protected molecules'. In the third class, the new molecules considered here have only the cluster core, and no ligand termination, and so are named 'exposed molecules'. This classification is illustrated in Fig. 1 for nickel chalcogenide systems, by NiS (the mineral millerite) as the non-molecular solid, by $[Ni_{11}S_8]$[12] as the exposed molecule and by $[Ni_{34}Se_{22}(PPh_3)_{10}]$[16] as the protected molecule. To illustrate again with the familiar carbon systems, diamond is non-molecular carbon, C_{60} is exposed molecular carbon, and the hydrocarbon dodecahedrane $C_{20}H_{20}$ represents protected C_{20}. This tripartite perspective is valuable and stimulates research in other fields of contemporary inorganic chemistry: some examples from metal–carbon systems are developed below. The concepts of non-molecularity, exposure and protection also pervade surface chemistry.

Metallocarbohedrenes

In 1992 a class of naked metal carbide clusters known as metallocarbohedrenes (or met-cars) was discovered.[17] These metallocarbohedrenes are synthesised when reactive metal clusters dehydrogenate hydrocarbons in the gas phase. The prototypical species was $[Ti_8C_{12}]^+$, but now more than a hundred metal–carbon molecules have been detected for metals

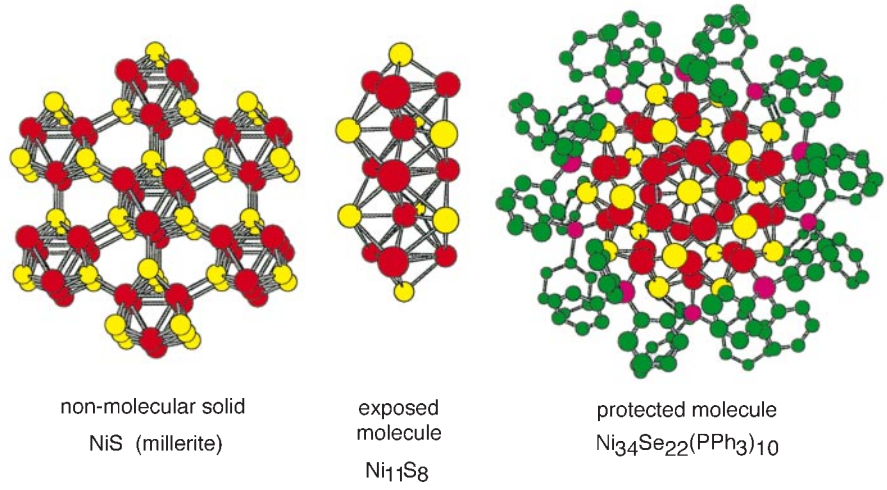

Fig. 1 Illustrations of the classification of non-molecular solids, exposed molecules, and protected molecules. Non-molecular NiS in the mineral millerite, the exposed molecule [$Ni_{11}S_8$] observed in the gas phase,[12] and the phosphine-protected nickel selenide core of [$Ni_{34}Se_{22}(PPh_3)_{10}$] prepared in solution and characterised crystallographically:[16] Ni red, S, Se yellow, P magenta, C green.

in groups 4–8 and 11. While many of these M_xC_y molecules have $y > x$ and an even number of C atoms and are believed to contain C_2 groups, there is a subset with $y \approx x$, believed to be fragments of a cubic metal carbide lattice containing C atoms.[18] The reactivities and transformations of metallocarbohedrenes are now well known,[18,19] but no pure bulk sample has been prepared. In the classification of Fig. 1, these exposed metal–carbon molecules lie between the non-molecular metal carbides[20] and organometallic clusters containing C_n moieties.[21]

Nitrogenase

Nitrogenase is the enzyme which reduces dinitrogen to ammonia, under conditions (ambient) which are far milder than those of the best industrial practice for reduction of N_2 with H_2 to form ammonia (the Haber–Bosch process, 400–500 °C, 100–1000 atm). The crystal structure of the FeMo protein of nitrogenase was determined in 1992, and subsequently improved,[22] revealing that the metal sulfide cluster (Fe_7MoS_9) at the active site is different from the many predictions, and unprecedented. The tantalising chemical question is 'how can a metal sulfide cluster enclosed in protein reduce one of the most recalcitrant molecules of chemistry under such mild conditions?' This question is another mantra in the philosophy of biognosis which holds that sophisticated chemistry can be learned from evolved biology.

The essential features of the Fe_7MoS_9 cluster at the active site are shown in Fig. 2. A six-coordinate Mo atom is coordinated by a side-chain histidine, bidentate homocitrate and three triply bridging sulfide ions to one triangular end of a trigonal prism of Fe atoms. The opposite end of this trigonal prism is connected through three triply bridging sulfides to the seventh Fe atom, whose tetrahedral coordination is completed by a cysteine residue. Around the equatorial belt of the trigonal prism there are three doubly-bridging sulfide ions. The significant features of the cluster are the threefold coordination of each of the six Fe^3 atoms† in the trigonal prism, the doubly-bridging S^2 atoms bridging the axial edges of the trigonal prism, and the connection of the cluster to the protein only at two end positions. The nakedness of the central Fe^3 and S^2 atoms is a conceptual link with the exposed metal sulfide clusters in the gas phase. Of course the essential Fe_7MoS_9 cluster is enclosed by protein, and the sophistication of the catalysis effected by nitrogenase depends on the cooperative action of cluster and protein, and the hydrogen bonds which link them. The Fe_7MoS_9 cluster participates in a rich sequence of reactions which probably depend, at least in part, on the reactivity of nakedness. There is another conceptual link between nitrogenase and the

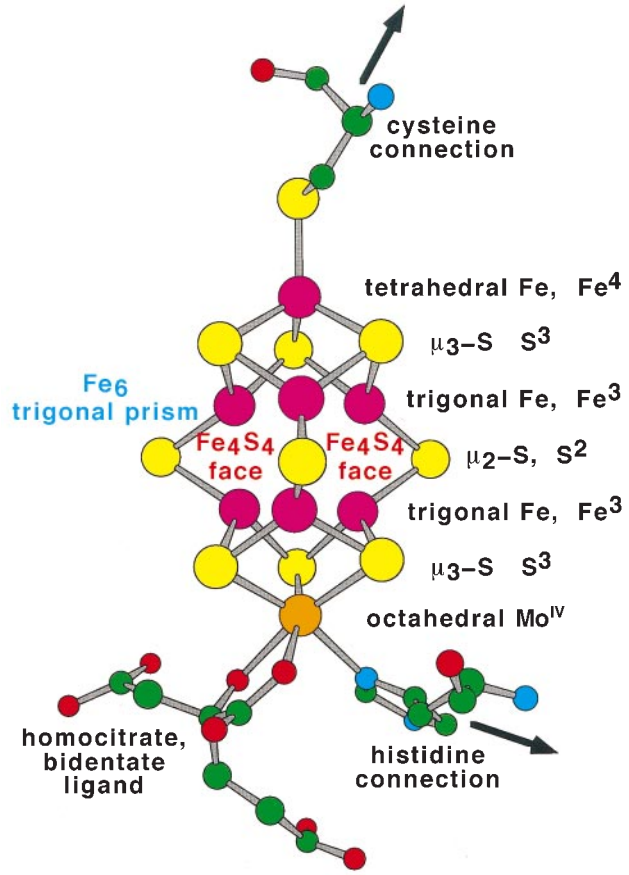

Fig. 2 The essential features of the Fe_7MoS_9(cysteine)(histidine)(homocitrate) cluster at the active site of the enzyme nitrogenase: Fe magenta, Mo orange, S yellow, C green, N blue, O red

gas phase metallocarbohedrene chemistry, in that the C_2^{2-} ligand of the metallocarbohedrenes is isoelectronic with the primary substrate N_2 of nitrogenase.

Determination of the crystal structure of the key protein of nitrogenase revealed the stage on which the marvellous molecular dance occurs, but provided no direct information about the dancers or the choreography.[23] The question now is how to determine that choreography.

Similar questions arise for the new exposed inorganic molecules. Their compositions and reactions are known mass

spectrometrically, but not their structures. In all of these contexts, powerful density functional theory provides valuable insights.

Calculating the structures and reactions of big molecules

Density functional theory (DFT) is now well established as a valuable quantum method for the calculation of the electronic structure and energy, and derived properties, of large molecules and molecules containing atoms which contribute many electrons.[11,24] DFT includes a computationally efficient account of the correlation and exchange energies (the electron–electron energies) which have complicated and prolonged traditional quantum chemical calculations. Apart from the selection of functionals to describe exchange and correlation, the DFT method is *ab initio*.

The performance of DFT calculations is impressive for molecules like those introduced above. For a calculational effort which scales with the number of electrons more favourably than any comparable method, optimised geometries are obtained with an accuracy sufficient to address the big-picture questions. As illustration, Fig. 3 shows the optimised structure of

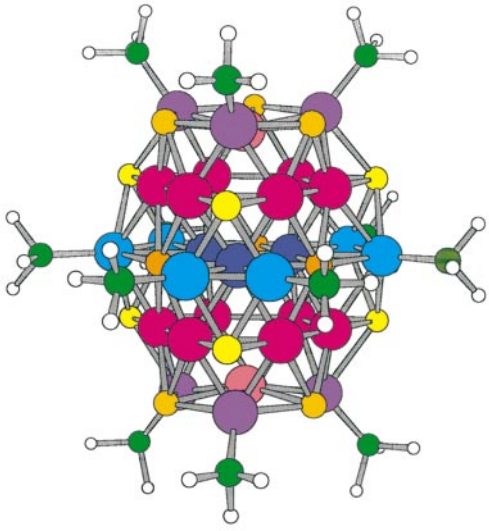

Bond	Obs	R=H: vwn/b88e
$Cu^h - Se^6$	2.56–2.62	2.52–2.56
$Cu^h - Se^4$	2.36–2.39	2.43, 2.44
$Cu^e - Se^4$	2.45–2.50	2.51, 2.52
$Cu^h - Se^5$	2.39–2.41	2.45, 2.46
$Cu^p - Se^5$	2.52–2.56	2.49–2.53
$Cu^a - Se^5$	2.48–2.53	2.55, 2.58
$Cu^h - Cu^h$	2.50–2.69	2.51–2.72
$Cu^h - Cu^p$	2.63–2.70	2.52–2.55
$Cu^p - Cu^a$	2.59–2.62	2.50, 2.51
$Cu^e - Cu^e$	2.63–2.74	2.52–2.56
$Cu^e - P$	2.23–2.26	2.23–2.25
$Cu^p - P$	2.22–2.25	2.20, 2.21

Fig. 3 The structure of $Cu_{29}Se_{15}(PR_3)_{12}$: large spheres are Cu atoms, colour coded according to chemical type and connectivity (point group D_{3h}), small yellow and orange spheres are Se, green P and white H. The tabulation of colour-coded bond types compares the distance range observed for R = Pr^i with the distances calculated (in C_{2v}) for R = H, using the Vosko–Wilke–Nusair local density functional[28] for correlation and Becke's gradient-corrected exchange functional.[29]

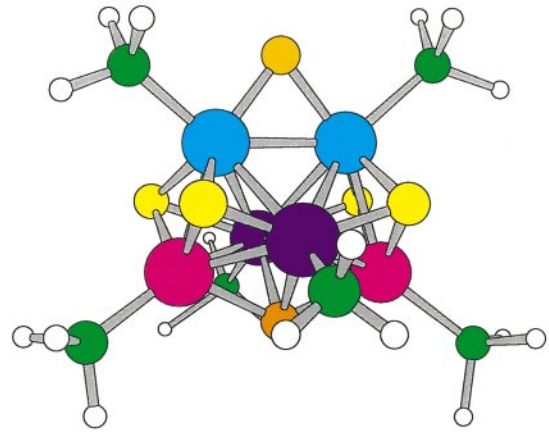

Bond	Obs	R=H: lyp/b88e
$Fe^a - S^2$	2.15	2.15
$Fe^a - S^3$	2.22, 2.23	2.20
$Fe^b - S^3$	2.19, 2.20	2.20
$Fe^c - S^3$	2.22	2.18
$Fe^c - S^4$	2.28, 2.30	2.25
$Fe^b - S^4$	2.23	2.19
$Fe^a - Fe^a$	2.63	2.62
$Fe^b - Fe^a$	2.72	2.73
$Fe^b - Fe^b$	2.97	3.00
$Fe^b - Fe^c$	2.63, 2.65	2.61
$Fe^a - P$	2.27, 2.29	2.32
$Fe^b - P$	2.28	2.31
$Fe^c - P$	2.36, 2.38	2.31

Fig. 4 The structure of $[Fe_6S_6(PR_3)_6]^{2+}$: large spheres are Fe atoms, colour coded according to chemical type and connectivity (point group C_{2v}), small yellow, light orange and deep orange spheres are S, green P and white H. The tabulation of colour-coded bond types compares the distances observed for R = Et with the distance calculated (in C_{2v}) for R = H, using the Lee–Yang–Parr gradient-corrected correlation functional[30] and Becke's gradient-corrected exchange functional.[29]

$Cu_{29}Se_{15}(PH_3)_{12}$ (which contains 1566 electrons) in comparison with the observed (X-ray crystal structure[25]) geometry for $Cu_{29}Se_{15}(PPr^i_3)_{12}$, and Fig. 4 shows the results for the 'basket cluster' $[Fe_6S_6(PR_3)_6]^{2+}$ (R = H calculated, R = Et observed[26]). In both molecules it can be seen that the calculated interatomic distances are generally within 0.05 Å (and often 0.02 Å) of those observed, and that the variability of bond type and length is reproduced, including long Fe–Fe distances which are not bonds. This augurs well for application to molecular metal sulfide clusters and to nitrogenase. There are extensive checks of calculated energies against experimental data.[27]

In exploring the geometry–energy hypersurface for new chemical systems it is also desirable to locate transition states (saddle points) and to calculate reaction profiles. The method used here is to postulate a saddle geometry, then follow the geometry change on its steepest downhill energy path, and then to iterate through a cycle of geometry adjustment and energy minimisation until the lowest energy transition state is found.

Answering the questions: transferring concepts

The new inorganic molecules and their reactions present innumerable questions. In DFT we have a powerful tool for answering those questions, or at least for the design of fruitful further experiments. The key challenge—and the exciting appeal of this research—is in devising the best hypotheses. In

my view the quality of research of this type is determined more by the quality of the ideas to be tested than by the computational methodology to be deployed.

In the following sections I outline some responses to the questions raised, with emphasis on the transferability of ideas and insight from metal sulfides to metallocarbohedrenes to nitrogenase, and the incorporation of structural data and principles from related non-molecular solids and protected molecules.

Structures of molecular metal sulfides

The compositions of the observed molecules $[M_xS_y]$ are plotted on maps of y *vs.* x, and show several significant general characteristics. Firstly, the x/y distribution is a continuous extended domain which is relatively narrow in y. In the case of $[Cu_xS_y]^-$, the main sequence of larger species can be described by the equations $x = 2y - 1$ and $x = 2y - 2$,[4,6] while for $[Mn_xS_y]^-$ the ions are described by $x = y$ and $x = y - 1$.[8] The continuous narrow regions of observability accentuate in contrast the emptiness of the composition maps and the many species which are not observed. Secondly, while for any metal there are variations in intensity along these sequences, there are no pronounced discontinuities in abundance which might signify special stability or structure. Thirdly, it must be remembered that observability on the composition map need not represent inherent stability, and could be due to favourable electron affinity in the competition for electrons during the formation of the anions. Fourthly, the slopes (y/x) of the domains of observability correlate with the number of valence electrons provided by M, and a qualitative electron counting pattern has been identified.[1,4]

The first issue for the new molecules is geometry: what is $[Mn_{20}S_{20}]^-$, or $[Fe_{11}S_{10}]^-$, or $[Co_{38}S_{24}]^-$, or $[Ni_{15}S_{10}]^-$, or . . .? And then, is there a fundamental structural principle for each metal? And are there structural principles which allow almost continuous growth, rather than special stability at certain sizes? In answering questions about geometry, knowledge of the many structures of terminally ligated metal chalcogenide clusters[2] provides inspiration for postulates to be tested.

In the case of $[Cu_xS_y]^-$ clusters, the enhanced stability of $[Cu_3S_3]^-$, $[Cu_6S_4]^-$ and $[Cu_{10}S_6]^-$ has been traced to cluster structures which contain local S–Cu–S linear (or near-linear) coordination, and the other reactive clusters are those which have exposed Cu atoms without this geometry.[4] For the $[Mn_xS_y]^-$ set,[8] 61 isomers for 23 compositions up to $[Mn_{15}S_{15}]^-$ have been evaluated by DFT in terms of optimised geometrical structure, electronic structure, and electron affinity.[7] Structures based on stacks of Mn_3S_3 triangles are favourable, as are regular Mn_x polyhedra with (μ_3-S) caps, and trigonal MnS_3 local coordination occurs in the more stable isomers.

Structures of metallocarbohedrenes

The prototypical metallocarbohedrene Ti_8C_{12} was postulated to have a structure (symmetry T_h) in which six C_2 units cap the faces of a Ti_8 cube, with the C_2 parallel to the edges of Ti_4 squares.[17] In this, the Ti–C and C–C bonds constitute a pentagonal dodecahedron, with analogy to C_{20}. My idea that there could be alternative stable structures came from a quite different field, metal thiolate clusters. The $M_8(SR)_{12}$ based clusters had been investigated earlier, when it was recognised that the M_8 polyhedron could be either a cube or a tetracapped tetrahedron, and that the bridging S atoms could constitute either a cuboctahedron or an icosahedron.[31,32] Therefore I explored alternatives for Ti_8C_{12}, and recognised a high symmetry (T_d) structure in which the Ti_8 set was a tetracapped tetrahedron, with the six C_2 groups bonded diagonally on each of the six folded Ti_4 rhombuses (or butterflies) on the Ti_8 surface (see Fig. 5). DFT calculations readily showed that the T_d structure was very much more stable than the T_h structure,[33] and this was confirmed by other theoretical investigations.[18,34] There are other isomers for M_8C_{12} which have lower symmetry arrangements of the diagonally bound C_2.[34] Subsequently I characterised the barrierless transformation of T_h-Ti_8C_{12} to T_d-Ti_8C_{12}, outlined in Fig. 5.[35]

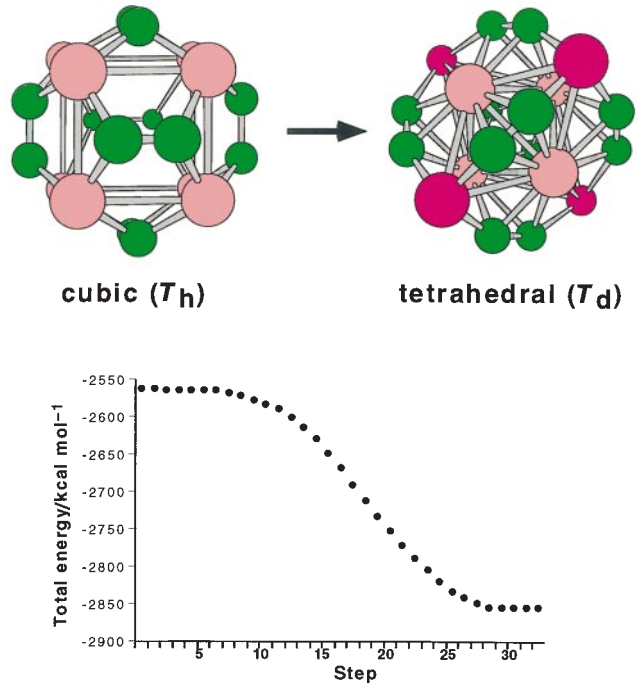

Fig. 5 The T_h and T_d isomers of Ti_8C_{12} (C green), and the barrierless energy change of 300 kcal mol^{-1} (1 cal = 4.184 J) in the transformation (in point group D_2) of T_h to T_d. In the T_d isomer the inner and outer Ti atoms are coloured pink and purple, respectively.

The concept of C_2 bonded diagonally across an M_4 rhombus rather than parallel to edges of an M_4 quadrilateral is entrenched in the models of many other metcars, such as the photodissociative transformation of $Ti_{14}C_{13}$ to Ti_8C_{13},[36] the structures of the unusual niobium carbohedrenes,[37] and the copper carbohedrenes.[38] Copper is unique in being the only late-transition metal reported to form metallocarbohedrenes: carbohedrenes are not known for metals in groups 9 or 10.

Copper carbohedrenes Cu_xC_y were observed in the series $[Cu_{2n+1}C_{2n}]^+$ for $1 \leqslant n \leqslant 10$, as well as $[Cu_7C_8]^+$, $[Cu_9C_{10}]^+$, $[Cu_{12}C_{12}]^+$, $[Cu_{16}C_{16}]^+$ and $[Cu_{20}C_{18}]^+$.[18] I noted a similarity between these compositions and those of the naked copper sulfide clusters $[Cu_xS_y]^-$, if C_2 was stoichiometrically equivalent to S. This similarity is shown on the composition map in Fig. 6. This is reasonable because both S^{2-} and C_2^{2-} can be isovalence-electronic in their bonding in metal clusters, both providing four donor electron pairs and having empty acceptor orbitals, as shown diagrammatically in Fig. 7.

Figs. 8 and 9 illustrate analogies between copper sulfide structures and copper carbohedrenes. The high symmetry structures of $Cu_{12}S_7$ (point group O_h) and $Cu_{13}(C_2)_6$ (point group T_h) have the same connectivity with either S or C_2 bound to the Cu_4 units of a cuboctahedron (see Fig. 8): the stoichiometry difference is accounted for by the presence of S at the centre of $Cu_{13}S_7$ and Cu at the centre of $Cu_{13}(C_2)_6$. This structural homology can be extended through larger clusters, to $Cu_{24}S_{13}$ and $Cu_{25}C_{24}$,[38] shown in Fig. 9.

While much further investigation is required to reveal the structures of the large numbers of exposed metal sulfide and metallocarbohedrene molecules, some guiding principles are becoming clear, and the analogies between the sulfide and carbide clusters stimulate hypotheses.

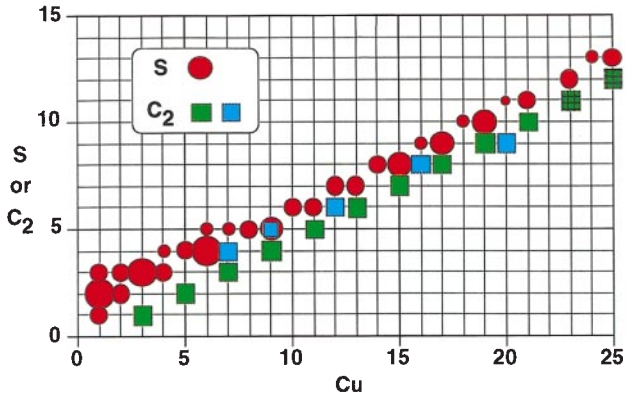

Fig. 6 Map of the compositions of $[Cu_xS_y]^-$ (red) and $[Cu_x(C_2)_y]^+$ (green, blue) in the gas phase: the vertical axis plots the number of S atoms or C_2 groups. The green compositions belong to the series $[Cu_{2n+1}C_{2n}]$, but the hatched green species were not observed.[18]

Fig. 7 Comparison (diagrammatic, not stereochemical) of the electronic components of sulfide S^{2-} and acetylide C_2^{2-} available for bonding participation in metal clusters. Both have four donor electron pairs marked as heavy lines (for C_2^{2-} these are the terminal σ pairs and the two π bonding pairs) and both have empty orbitals marked as lobes, being d orbitals at S and π* orbitals on C_2^{2-}: not all of these empty orbitals are shown.

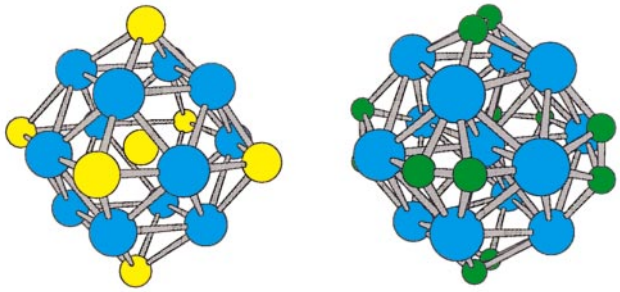

Fig. 8 Comparison of the optimised structures of $[Cu_{12}S_7]$ and $[Cu_{13}(C_2)_6]^+$, in which S and C_2 groups interchangeably cap the faces of a Cu_{12} cuboctahedron

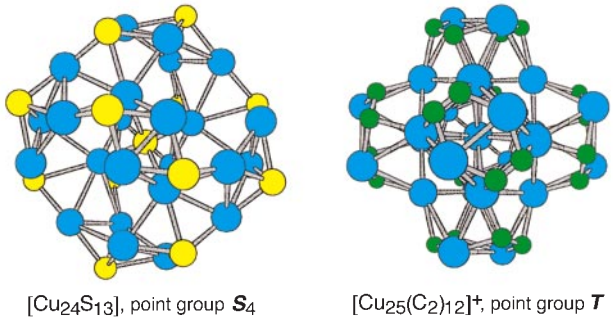

Fig. 9 Comparison of the optimised structures for $Cu_{24}S_{13}$ and $[Cu_{25}(C_2)_{12}]^+$, in which S and C_2 groups occupy similar positions on the surface of a Cu_{24} framework which is a distorted hexacapped cuboctahedron. The differences are due to tetrahedral coordination of the central S in $Cu_{24}S_{13}$ but cuboctahedral coordination of the central Cu in $[Cu_{25}(C_2)_{12}]^+$.

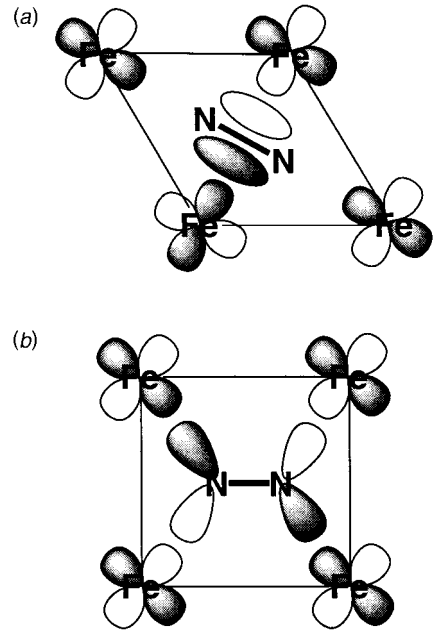

Fig. 10 Hypotheses for N_2 binding to an $(Fe^3)_4$ face of the Fe_7MoS_9 cluster of nitrogenase. (*a*) The twist or rhombus configuration allowing overlap between the Fe orbitals and N_2 π-bonding orbitals. (*b*) The parallel or rectangle configuration in which the Fe orbitals overlap with N_2 π-antibonding orbitals.

Tantalising nitrogenase

As already mentioned, the structure of the resting FeMo protein revealed nothing about the mechanism for conversion of N_2 to NH_3. There is however a very large amount of data on the kinetics and spectroscopy (mainly EPR) of the enzyme with various substrates and inhibitors, impressive model chemistry, and information about the effects of site-directed mutations.[22,39] An issue is how to incorporate the new structural data into a more detailed and chemical description of the mechanism. More specifically there are questions about the location and geometry for the initial binding of N_2, the bonding geometry which activates N_2, the effects of introduction of electrons, the proton approach pathways, details of the binding of the intermediates, and the pathway for egress of products. Nitrogenase reduces protons in amounts determined by the availability of N_2, and H_2 inhibits N_2 reduction, and so there are related key questions about the binding of H^+, H and H_2 at the active site.

The first question (although not necessarily the first step in the mechanism) concerns the binding of N_2. In 1993, a lecture by Doug Rees about the cluster structure triggered the idea that the metallocarbohedrene experience was relevant. The hypothesis was:[40]

(*i*) metallocarbohedrenes have C_2 bound most stably along the long diagonal of a M_4 rhombus, while C_2 bonding parallel to the edges of an M_4 rectangle is less stable;
(*ii*) the $(Fe^3)_6$ trigonal prism of nitrogenase has three $(Fe^3)_4$ rectangular faces;
(*iii*) rotation of a trigonal prism about its threefold axis changes the rectangular faces to rhombuses;
(*iv*) N_2 is isoelectronic with C_2^{2-};
(*v*) therefore the N_2 could be bound stably to an $(Fe^3)_4$ rhombus face of a twisted form of the $(Fe^3)_6$ trigonal prism [Fig. 10(*a*)];
(*vi*) rotation back to the trigonal prismatic $(Fe^3)_6$ geometry with a rectangular $(Fe^3)_4$ face could weaken the N–N bond [Fig. 10(*b*)], which is the objective.

This hypothesis was fully consistent with the binding of the Fe_7MoS_9 cluster to the protein, because the cluster is anchored at the six-coordinate Mo end, but able to rotate the other end

about the pseudo-threefold axis coincident with the Fe–S_{cys} bond.

The feasibility of an $(Fe^3)_4$ face of the cluster as N_2 binding site was developed by examination of the protein surrounds and hydrogen bonds, revealing that the $(Fe^3)_4$ face capped by the extended side chain of arginine-359 was much better positioned than the other two for substrate binding:[79] this full $[(Fe^3)_4(S^2)_2(S^3)_2]$ face proposed for action is named the front face. DFT calculations demonstrated the feasibility of N_2 binding at this face, and also revealed that reduction of the cluster concentrated negative electron density on the S (rather than Fe or Mo) atoms, and particularly on the S^2 atoms flanking the binding face. Since these two flanking S^2 atoms are hydrogen bonded to protein from behind the front face, this result inspired the important mechanistic concept of proton transfer to bound substrate *via* these S^2 atoms according to their redox-moderated basicity, along the pathway illustrated in Fig. 11.

Continued application of DFT to the questions about nitrogenase structure and mechanism has provided further insight[41] into: (*a*) the flexibility of the Fe_7MoS_9(cys)(his)(cit) core structure; (*b*) the influence of redox level (both electronation and hydrogenation) on the geometry of the core; (*c*) the optimum geometries for N_2 bound to the core in various ways, and their relative energies; (*d*) the sliding of H atoms around the cluster atoms, in relation to the $2e^- + 2\,H^+ \rightleftharpoons H_2$ processes and the exchangeable and non-exchangeable hydrogen binding sites; (*e*) the binding of inhibitor CO and alternative substrates; and (*f*) the formation of NH_3.

The initial idea of the trigonal prism twisting about its threefold axis has been expanded to include and explore all of the conformational freedom of the Fe_7MoS_9 cluster. Because this cluster is undercoordinated it was expected to be floppy. Using the distortions shown in Fig. 12, DFT calculations with the 38-atom asymmetric model (Fig. 12) show that the energy surface for these distortions is relatively flat. Variations of Fe–Fe distances by up to 1 Å involve energy changes of < 10 kcal mol^{-1}: the flatness of the energy surface is dependent on the redox level.

A number of geometries for N_2 binding to the Fe_7MoS_9 cluster have been investigated theoretically.[40,42] My DFT calculations show that terminal η^1 binding of N_2 to one of the Fe^3 atoms is energetically favourable, and draws the Fe^3 atom out of the cluster to achieve local trigonal pyramidal coordination. However this does not elongate N–N as much as does η^2, μ_4 binding of both N atoms of N_2 to an $(Fe^3)_4$ face. The lowest energy η^2, μ_4 geometry is the conformation shown in Fig. 13(*left*), and dubbed 'oblique arrow' to describe the approach of N_2 to the $(Fe^3)_4$ face. One N atom, labelled $N^{proximal}$, is bonded to all four Fe^3 atoms, while the other (N^{distal}) is bonded to two Fe^3. This configuration is *ca.* 27 kcal mol^{-1} more stable than the symmetrical configuration of Fig. 13(*right*), and the N–N bond in the oblique arrow geometry is 1.29 Å relative to 1.10 Å in free N_2. The 'direct arrow' configuration in which N_2 is bound symmetrically to $(Fe^3)_4$ through only one N atom is not an energy minimum.

The N^{distal} atom in the oblique arrow conformation is positioned between three S atoms (two S^3, one S^2) on the front face, with N···S distances of 2.7–3.0 Å. Electronation of the cluster is calculated to increase the basicity of these S atoms, allowing H^+ ions to be transferred to them *via* hydrogen bonds, and after inversion at S^2 the resulting bound H atoms are within hydrogen bonding distance of the N^{distal} atom. This suggested a

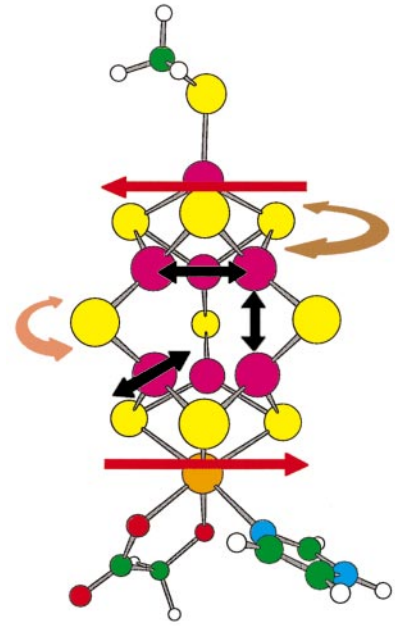

Fig. 12 Conformational freedom of the Fe_7MoS_9(cys)(his)(cit) cluster. The red arrows represent lateral shear, the brown arrow represents torsional twist about the pseudo-threefold axis, the orange arrow represents flapping of the S^2 atoms, and the black arrows represent various expansions and/or contractions of the $(Fe^3)_6$ trigonal prism.

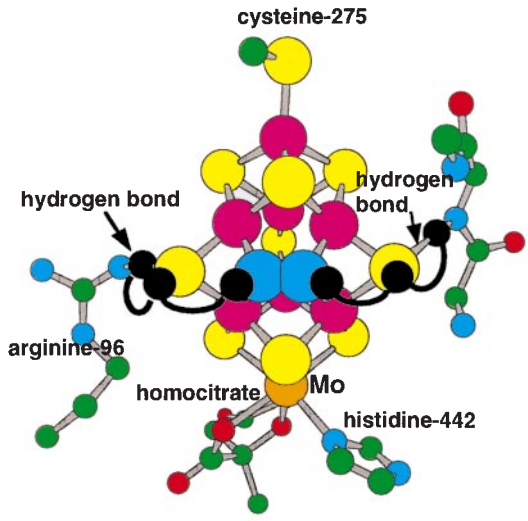

Fig. 11 The Fe_7MoS_9(cysteine)(histidine)(homocitrate) cluster, showing hydrogen bonds from behind the S^2 atoms flanking the front face, and the postulated transfer of H to bound N_2 by inversion of (S^2–H)

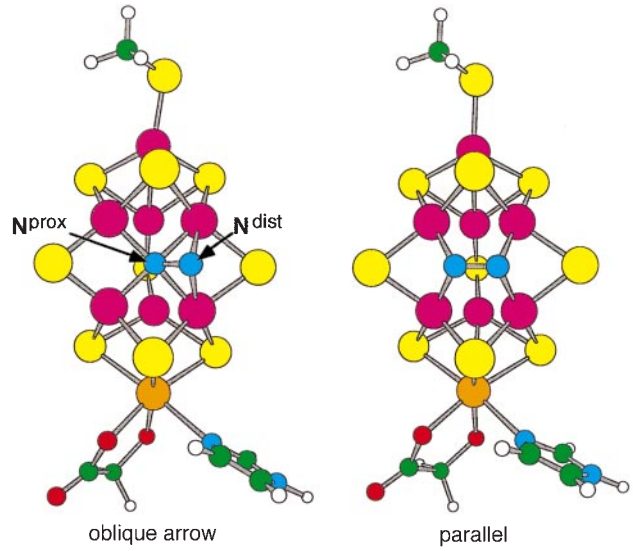

Fig. 13 The oblique arrow and parallel binding geometries for N_2 on the $(Fe^3)_4$ face of the Fe_7MoS_9(cys)(cit)(his) cluster. The calculated N–N distances are 1.29 and 1.25 Å, respectively.

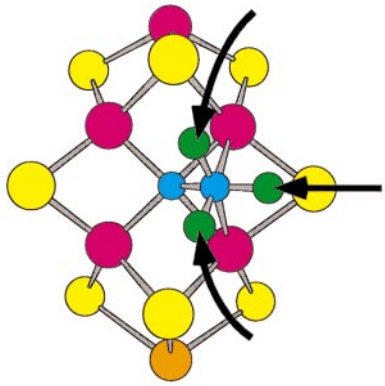

Fig. 14 Part of the front face of the Fe_7MoS_9(cys)(his)(cit) cluster showing N_2 bound in the oblique arrow configuration, the proposed trajectories for protonation of N^{distal}, and the H atom locations in the postulated transition state

mechanism for hydrogenation of N^{distal}. The transition state shown in Fig. 14 for transfer of these H atoms to N^{distal} was postulated, and on energy minimisation the N–N bond broke and NH_3 formed as N^{distal} separates.[43] This process is calculated to be exergonic by many tens of kcal mol^{-1}. Similar protonation of $N^{proximal}$ *via* the closest S atoms, in concert with electronation *via* the cluster, is postulated for subsequent formation of the second NH_3 product.[43]

The chemistry of hydrogen at the active site, while not as dramatic as the breaking of a very strong triple bond, is almost as intriguing. Some facts[39] are that proton reduction always accompanies N_2 reduction, in amounts depending on the availability of N_2; $H_{2\,(g)}$ inhibits N_2 reduction; the reductive formation of $HD_{(g)}$ from protons in the presence of $D_{2\,(g)}$ occurs in the presence of N_2 and with the same kinetics as N_2 reduction. A mechanistic requirement is that H atoms from the gas phase must always remain distinguishable from H atoms from water.[39]

The bonding and sliding of H atoms over the Fe and S atoms of the cluster can be investigated by DFT. One result is that H atoms bound to S atoms weaken their ligating ability, lengthening Fe^3–S bonds and shortening Fe^3–Fe^3 distances, while H atoms bonded to Fe^3 lengthen Fe^3–Fe^3 distances.[41] Other calculations show how H_2 can bind to Fe. Various $2H \rightleftharpoons H_2$ interconversions on the Fe_7MoS_9 cluster can be demonstrated.[41] As an illustration of the type of calculation which can inform this cluster–hydrogen chemistry, Fig. 15 outlines the main features of a calculated reaction coordinate for a symmetrical $2(S^2\text{–}H) \rightleftharpoons H_2$ interconversion on a $Fe_8S_9(SMe)_2$ model.

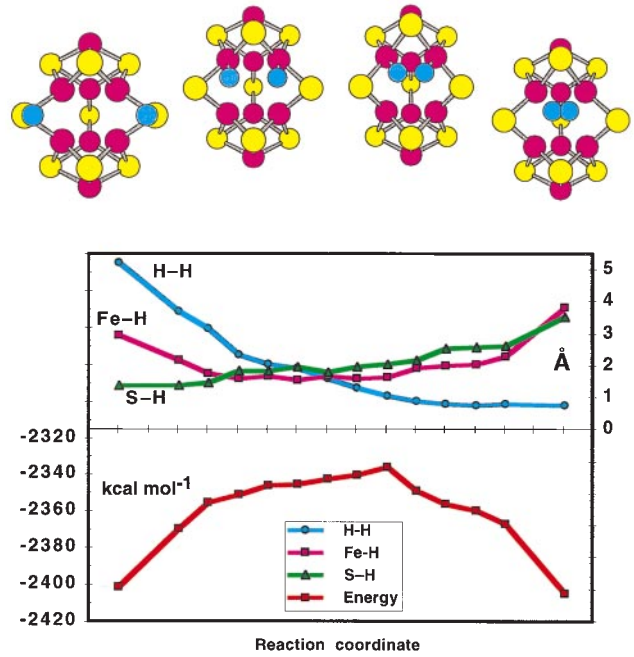

Fig. 15 Calculated reaction coordinate for a $2(S^2\text{–}H) \rightleftharpoons H_2$ transformation occurring on an $Fe_8S_9(SMe)_2$ model with C_s symmetry. Four structures in the sequence are shown at the top (with SMe groups omitted): in the left diagram two H atoms (blue) are bound to S^2 atoms, then move together *via* the mediation of Fe^3–H bonds, and then form H_2 which separates from the cluster. Interatomic distances and total energy through 14 points around the transition state are presented in the box.

Prospectives

This short account has provided glimpses of (1) the new chemistry which occurs for unprotected fundamental inorganic molecules, (2) consideration of this new molecular chemistry in the context of the more familiar non-molecular and protected analogous compounds, (3) the value of DFT, and (4) the value of concept-transfer between rather different chemical systems. But overall this has raised more questions than answers, and so I conclude with some prospectives for further research.

Continuing investigations of the formation and reactions of fundamental inorganic molecules in the gas phase, free of the ameliorating influences of solvation or crystal surrounds, will reveal more rule-breakers and expand the conceptual basis of fundamental inorganic chemistry.

A key objective is the preparation of bulk samples of the new molecules: this can be approached by condensation from the gas phase (*cf.* the fullerenes), or by planned reactions in relatively inert solution. The preparation of phosphine-protected copper sulfide clusters inspired by the gas phase results has been reported.[44] Preparation from the gas phase is likely to require condensation into a milieu which is inert or contains protecting ligands, to restrict conversion to non-molecular solids. On the basis of observed reactivities in the gas phase, the demonstrated successes of Dehnen and Fenske[44] using protecting ligands, and the calculated correlations of structure and reactivity, copper appears to be the most promising metal for preparation of the new molecules.

The Fe_7MoS_9 molecule at the catalytic site of nitrogenase is unprotected, in the sense of being undercoordinated, and is calculated to be reactive like other exposed metal sulfide molecules. It is also calculated to be floppy. The Fe_7MoS_9 cluster probably requires its protein cage for restraint of distortions, as well as restraint of some reactivity. The concerted enhancement of the catalytic reactivity of the Fe_7MoS_9 molecule by the protein surrounds is likely to occur primarily through the S atoms.

In an experimentally complex system such as the active site of nitrogenase, powerful DFT methods can provide insight and guidance to the experimental program.

Acknowledgments

I thank my coworkers and colleagues named in the references for their experimental efforts, vigorous discussions, and provision of information in advance of publication. This research is funded by the Australian Research Council and the University of NSW, and the Australian Nuclear Science and Technology Organisation provided computational resources.

Ian Dance is Professor of Inorganic Chemistry at the University of New South Wales. His formative research was under the direction of Professors Hans Freeman (Sydney), Jack Lewis (Manchester) and Richard Holm (MIT). He served on the faculty of the University of Wisconsin, Madison before joining the University of New South Wales in 1975. He won the Inorganic Award of the Royal Australian Chemical Institute in

1996, and was elected to Fellowship of the Australian Academy of Science in 1997.

Notes and References

* E-mail: i.dance@unsw.edu.au

† In the notation E^n the superscript *n* is the coordination number of E.

1 J. H. El Nakat, K. J. Fisher, I. G. Dance and G. D. Willett, *Inorg. Chem.*, 1993, **32**, 1931.
2 I. G. Dance and K. J. Fisher, *Prog. Inorg. Chem.*, 1994, **41**, 637.
3 I. G. Dance and K. J. Fisher, *Mater. Sci. Forum*, 1994, **152**, 137.
4 K. J. Fisher, I. G. Dance, G. D. Willett and M. Yi, *J. Chem. Soc., Dalton Trans.*, 1996, 709.
5 H. J. El-Nakat, I. G. Dance, K. J. Fisher and G. D. Willett, *J. Chem. Soc., Chem. Commun.*, 1991, 746.
6 J. H. El Nakat, I. G. Dance, K. J. Fisher and G. D. Willett, *Inorg. Chem.*, 1991, **30**, 2957.
7 I. G. Dance and K. J. Fisher, *J. Chem. Soc., Dalton Trans.*, 1997, 2563.
8 I. G. Dance, K. J. Fisher and G. D. Willett, *J. Chem. Soc., Dalton Trans.*, 1997, 2557.
9 K. Fisher and I. G. Dance, *J. Chem. Soc., Dalton Trans.*, 1997, 2381.
10 K. J. Fisher, I. G. Dance and G. D. Willett, *Polyhedron*, 1997, **16**, 2731.
11 I. G. Dance, in *Transition Metal Sulfur Chemistry: Biological and Industrial Significance*, ed. E. I. Stiefel and K. Matsumoto, American Chemical Society, Washington, DC, 1996, pp. 135–152.
12 J. H. El Nakat, I. G. Dance, K. J. Fisher, D. Rice and G. D. Willett, *J. Am. Chem. Soc.*, 1991, **113**, 5141.
13 K. J. Fisher, I. G. Dance and G. D. Willett, *Rapid Commun. Mass Spectrom.*, 1996, **10**, 106.
14 I. G. Dance, K. J. Fisher and G. D. Willett, *Inorg. Chem.*, 1996, **35**, 4177.
15 I. G. Dance, K. J. Fisher and G. D. Willett, *J. Chem. Soc., Chem. Commun.*, 1995, 975.
16 D. Fenske, J. Ohmer and J. Hachgenei, *Angew. Chem., Int. Ed. Engl.*, 1985, **24**, 993.
17 B. C. Guo, K. P. Kerns and A. W. Castleman, *Science*, 1992, **255**, 1411; A. W. Castleman, B. C. Guo, S. Wei and Z. Y. Chen, *Plasma Phys. Controlled Fusion*, 1992, **34**, 2047; Z. Y. Chen, G. J. Walder and A. W. Castleman, *J. Phys. Chem.*, 1992, **96**, 9581; S. Wei, B. C. Guo, J. Purnell, S. Buzza and A. W. Castleman, *Science*, 1992, **256**, 818.
18 J. S. Pilgrim and M. A. Duncan, *J. Am. Chem. Soc.*, 1993, **115**, 6958; Y. Yamada and A. W. Castleman, *Chem. Phys. Lett.*, 1993, **204**, 133; A. W. Castleman and K. H. Bowen, *J. Phys. Chem.*, 1996, **100**, 12 911; M. M. Rohmer, M. Benard and J. M. Poblet, in *Metal Clusters in Chemistry*, ed. P. Braunstein, VCH-Wiley, New York, 1997, in press; J. S. Pilgrim and M. A. Duncan, *Adv. Met. Semicond. Clusters*, 1995, **3**, 181; J. S. Pilgrim and M. A. Duncan, *J. Am. Chem. Soc.*, 1993, **115**, 9724; J. S. Pilgrim and M. A. Duncan, *Int. J. Mass Spectrom Ion Process.*, 1994, **138**, 283.
19 C. S. Yeh, S. Afzaal, S. A. Lee, G. Byun and B. S. Freiser, *J. Am. Chem. Soc.*, 1994, **116**, 8806; Y. G. Byun and B. S. Freiser, *J. Am. Chem. Soc.*, 1996, **118**, 3681; H. T. Deng, K. P. Kerns and A. W. Castleman, *J. Am. Chem. Soc.*, 1996, **118**, 446; B. C. Guo, K. P. Kerns and A. W. Castleman, *J. Am. Chem. Soc.*, 1993, **115**, 7415; H. T. Deng, B. C. Guo, K. P. Kerns and A. W. Castleman, *J. Phys. Chem.*, 1994, **98**, 13 373.
20 R. B. King, *J. Organomet. Chem.*, 1997, **536**–**537**, 7.
21 C. J. Adams, M. I. Bruce, B. W. Skelton and A. H. White, *J. Chem. Soc., Chem. Commun.*, 1993, 446; C. J. Adams, M. I. Bruce, B. W. Skelton and A. H. White, *Chem. Commun.*, 1996, 969; T. Bartik, B. Bartik, M. Brady, R. Dembinski and J. A. Gladysz, *Angew. Chem., Int. Ed. Engl.*, 1996, **35**, 414; W. Weng, T. Bartik and J. A. Gladysz, *Angew. Chem., Int. Ed. Engl.*, 1994, **33**, 2199.
22 J. Kim and D. C. Rees, *Nature*, 1992, **360**, 553; M. M. Georgiadis, H. Komiya, P. Chakrabarti, D. Woo, J. J. Kornuc and D. C. Rees, *Science*, 1992, **257**, 1653; J. Kim and D. C. Rees, *Science*, 1992, **257**, 1677; D. C. Rees, M. K. Chan and J. Kim, *Adv. Inorg. Chem.*, 1993, **40**, 89; J. T. Bolin, A. E. Ronco, T. V. Morgan, L. E. Mortenson and N. H. Xuong, *Proc. Nat. Acad. Sci. USA*, 1993, **90**, 1078; M. K. Chan, J. Kim and D. C. Rees, *Science*, 1993, **260**, 792; J. B. Howard and D. C. Rees, *Chem. Rev.*, 1996, **96**, 2965; J. W. Peters, M. H. B. Stowell, S. M. Soltis, M. G. Finnegan, M. K. Johnson and D. C. Rees, *Biochem.*, 1997, **36**, 1181.
23 R. J. Deeth, *New Sci.*, July 5, 1997, 24.
24 B. B. Laird, R. B. Ross and T. Ziegler, *Chemical Applications of Density Functional Theory*, American Chemical Society, Washington, DC, 1996; R. J. Deeth, *Struct. Bonding* (*Berlin*), 1995, **82**, 1; L. Fan and T. Ziegler, in *Density Functional Theory of Molecules, Clusters and Solids*, ed. D. E. Ellis, Kluwer, Dordrecht, 1995, pp. 67–95.
25 D. Fenske, H. Krautscheid and S. Balter, *Angew. Chem., Int. Ed. Engl.*, 1990, **29**, 796.
26 B. S. Snyder and R. H. Holm, *Inorg. Chem.*, 1990, **29**, 274.
27 A. C. Scheiner, J. Baker and J. W. Andzelm, *J. Comput. Chem.*, 1997, **18**, 775.
28 S. H. Vosko, L. Wilke and M. Nusair, *Can. J. Phys.*, 1980, **58**, 1200.
29 A. D. Becke, *Phys. Rev. A*, 1988, **38**, 3098.
30 C. Lee, W. Yang and R. G. Parr, *Phys. Rev. B*, 1988, **37**, 785.
31 I. G. Dance, *Aust. J. Chem.*, 1985, **38**, 1391.
32 I. G. Dance, *Polyhedron*, 1986, **5**, 1037.
33 I. G. Dance, *J. Chem. Soc., Chem. Commun.*, 1992, 1779.
34 M. M. Rohmer, M. Benard, C. Henriet, C. Bo and J. M. Poblet, *J. Chem. Soc., Chem. Commun.*, 1993, 1182; M. M. Rohmer, M. Benard, C. Bo and J. M. Poblet, *J. Am. Chem. Soc.*, 1995, **117**, 508; L. Lou, T. Guo, P. Nordlander and R. E. Smalley, *J. Chem. Phys.*, 1993, **99**, 5301.
35 I. G. Dance, *J. Am. Chem. Soc.*, 1996, **118**, 6309.
36 I. G. Dance, *J. Am. Chem. Soc.*, 1996, **118**, 2699.
37 I. G. Dance and H. H. Harris, *17th International Conference on Organometallic Chemistry*, Brisbane, Australia, 1996, Abstract PA65.
38 I. G. Dance, *J. Chem. Soc., Chem. Commun.*, 1993, 1306; I. G. Dance, *J. Am. Chem. Soc.*, 1993, **115**, 11 052.
39 B. K. Burgess, *Chem. Rev.*, 1990, **90**, 1377; G. J. Leigh, *New J. Chem.*, 1994, **18**, 157; G. J. Leigh and C. N. McMahon, *J. Organomet. Chem.*, 1995, **500**, 219; G. J. Leigh, *Eur. J. Biochem.*, 1995, **229**, 14; J. W. Peters, K. Fisher and D. R. Dean, *Annu. Rev. Microbiol.*, 1995, **49**, 335; G. J. Leigh, in *Nitrogen Fixation: Fundamentals and Applications*, ed. A. Tikhonavich *et al.*, Kluwer Academic, Dordrecht, 1995, pp. 129–135; B. K. Burgess and D. J. Lowe, *Chem. Rev.*, 1996, **96**, 2983 and references therein; R. H. Holm, P. Kennepohl and E. I. Solomon, *Chem. Rev.*, 1996, **96**, 2239; D. Sellmann and J. Sutter, *J. Biol. Inorg. Chem.*, 1996, 587; R. R. Eady, *Chem. Rev.*, 1996, **96**, 3013; C. J. Pickett, *J. Biol. Inorg. Chem.*, 1996, **1**, 601; R. N. F. Thorneley and D. J. Lowe, *J. Biol. Inorg. Chem.*, 1996, **1**, 576.
40 I. G. Dance, *Aust. J. Chem.*, 1994, **47**, 979.
41 I. G. Dance, in preparation.
42 H. Deng and R. Hoffmann, *Angew. Chem., Int. Ed. Engl.*, 1993, **32**, 1062; W. Plass, *J. Mol. Struct.*, 1994, **315**, 53; I. G. Dance, *J. Biol. Inorg. Chem.*, 1996, **1**, 581; K. K. Stavrev and M. C. Zerner, *Chem. Eur. J.*, 1996, **2**, 83.
43 I. G. Dance, *Chem. Commun.*, 1997, 165.
44 S. Dehnen, A. Schafer, D. Fenske and R. Ahlrichs, *Angew. Chem., Int. Ed. Engl.*, 1994, **33**, 746; S. Dehnen and D. Fenske, *Chem. Eur. J.*, 1996, **2**, 1407; S. Dehnen and D. Fenske, *Angew. Chem., Int. Ed. Engl.*, 1994, **33**, 2287.

7/08218E